ISSN 2320 2599
Volume 2, No.1, January – February 2013
International Journal of Microwaves Applications
Available Online at http://warse.org/pdfs/2013/ijma07212013.pdf

Performance Improvement Study of Relativistic Magnetron Primings

Shivendra Maurya, V.V.P. Singh and P.K. Jain[1] SM IEEE
Council of Scientific and Industrial Research-Central Electronics Engineering Research Institute (CSIR-CEERI), Pilani-333 031
[1] IIT (BHU), Varanasi, INDIA
Email: shivendra_maurya@rediffmail.com

ABSTRACT

A three dimensional particle-in-cell (PIC) code MAGIC-3D has been used to study the output performance of a relativistic magnetron in combined effect of electric field priming and RF magnetic field perturbations. The side resonators of the resonant structure have been loaded symmetrically at angle of 120^0 with low-loss dielectric material in the form of annular section alternating with protrusions/recessions along anode vane inner surfaces to implement the electric field priming. The 3-symmetrical metal rods at angle of 120^0 in side resonators have been used to perturb the RF magnetic field as well as tuning the frequency of oscillation. All the simulations have been performed for 2π-mode of operation on the well known A6 relativistic magnetron. The results indicate that single 2π-mode operation is not possible with such combination of electric field priming and magnetic field perturbation by dielectric loading, protrusions/recession and insertion of metal rods simultaneously.

Key words: High power microwaves, MAGIC-3D, particle-in-cell (PIC) code, relativistic magnetron

1. INTRODUCTION

A magnetron is known as a high-efficient, high power and low cost device for generating microwaves from kW to GW-level at centimeter wavelength [1]. Because high power microwaves with long pulse length are important to the Department of Defense and the plasma physics research community, there is continued interest in improving the performance of relativistic magnetrons [2]. The output parameters of the relativistic magnetron that need to be improved include mode control, peak power, start oscillation time and pulse length [3]. One technique that has been used by several researchers world wide to improve the performance of the magnetron is "priming" [4-9]. The improvement in the case of oven and relativistic magnetron by magnetic priming has been published [6-7]. Another technique to improve the efficiency of the relativistic magnetron is with axial extraction of radiation through a horn antenna. The improvement demonstrated is up to 70% at gigawatt radiation power for an applied voltage of 400kV [10]. One of the recent techniques that have been published in the literature to improve mode
purity is to use partially dielectric filled side resonators [11]. The improvement in the radiated output power and efficiency by partially dielectric loaded cavities has been already demonstrated by us using PIC simulation code MAGIC-3D for A6 relativistic magnetron oscillating in 2π-mode [12]. We have also demonstrated fast oscillation startup and efficiency improvement in A6 relativistic magnetron through electric field priming by anode vanes shape modifications [13].

In this paper we use a three dimensional particle-in-cell code called MAGIC-3D to study the output performance of the A6 relativistic magnetron loaded symmetrically with low loss annular dielectric material alternating metal rods in side resonators and protrusions / recessions along anode vanes inner surfaces for 2π-mode of oscillation. The A6 relativistic magnetron is one of the most matured HPM sources. The resonant structure of this magnetron consists of six cavities with an azimuthal spacing of 60 degrees. The radius of cathode (r_c) and radius of anode (r_a) are 15.8 mm and 21.2 mm respectively. The vane inner radius (r_v) is 41.1 mm. The cross sectional view of A6 relativistic magnetron is as shown in figure 1.

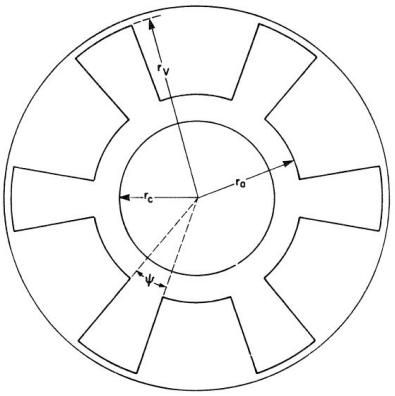

Figure 1: Resonant structure of a Relativistic magnetron

2. SIMULATION MODEL

MAGIC-3D is a user-configurable code that self-consistently solves the full set of time dependent Maxwell's equation and the complete Lorentz force equation to provide the interaction between space charge and electromagnetic fields [14]. A variety of 3D algorithms are

available for problem-specific solutions. For better accuracy and reduced simulation time we use the localized meshing technique [14]. In this simulation we have used explosive emission cathode model of the MAGIC-3D algorithms. Radiated output power is coupled from one of the side resonators by connecting a smooth tapered waveguide to the resonator as shown in figure 2(a). For modeling of the simulation modes polar coordinate system (r, θ, z) has been used. Figures 2(a) and (b) shows cross sectional views of the resonant structure symmetrically loaded with annular section dielectric alternating symmetrical recessions on anode vanes inner surfaces and metal rods in rθ and rz-plane respectively. The annular section dielectric material is filled up to 50% of the total depth of the side resonator and the optimized radius of the metal rod is 3mm. The optimized angular width of the recession / protrusions is 6^0 and their radial depth is 1.6 mm.

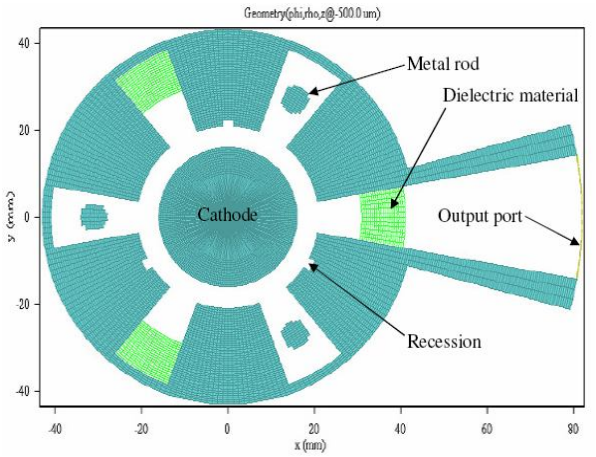

Figure 2 (a): Cross section of simulation model in rθ-plane

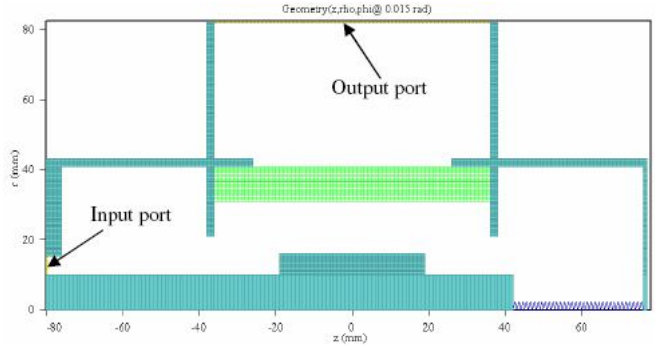

Figure 2 (b): Cross section of simulation model in rz-plane

As all cavities are tightly coupled to one another we can extract the output power from a single cavity. The cathode is also included in the simulation model to supply the required emission current. End caps are included in the model to prevent the axial escaping of electron, as axially escaped electron play no role in beam-wave interaction and decreases the efficiency of magnetron.

3. SIMULATION RESULTS

Before simulation of non-linear beam-wave interactions, electromagnetic simulations using the proposed geometries as well as A6 basic model have been carried out. The RF electric and magnetic field contour plots for the A6 basic resonant structure are as shown in figures 3(a) and (b) respectively. It is clear that the electric and magnetic contour plots in this case are uniform and symmetrical. The resonant frequency for A6 basic resonant structure was found to be 4.58GHz for 2π-mode of oscillation as shown on the top of figure 3.

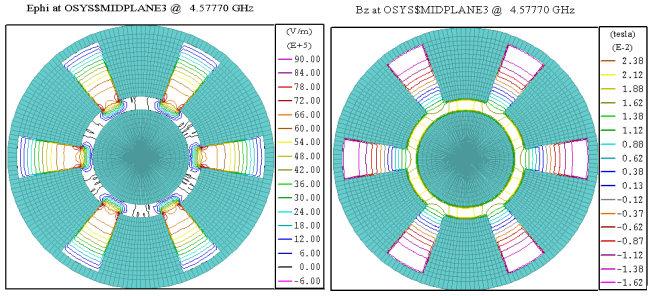

Figure 3: (a) RF Electric field (E_φ), and **(b)** RF magnetic field (B_z) contour plot of A6 basic resonant structure for 2π-mode of oscillation

Next, the electromagnetic simulation has been carried out on the model having 3-symmetrical annular section dielectric alternating protrusions/recession and metal rods in the side RF resonators. The corresponding electric and magnetic field contour plots are shown in figures 4(a) and (b) respectively. It is clear from figure 4 that azimuthal variation of RF electric and magnetic field in this case in non-uniform and asymmetric. The resonant frequency for this case is found to be 4.448 GHz. Hence there is a downward frequency shift of 132 MHz as compared to the A6 basic resonant structure.

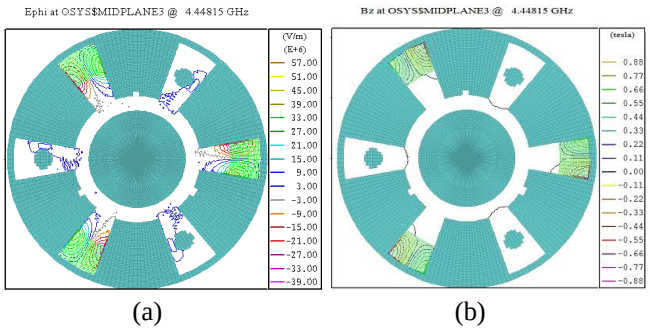

Figure 4: Azimuthal variation of **(a)** RF electric field (b) RF magnetic field for 2π-mode of oscillation with annular dielectric loaded RF resonators alternating 3 metal rods and recessions

Electromagnetic simulation has been also carried out on the model having annular dielectric loaded RF resonators alternating 3 metal rods and protrusions. The RF electric and magnetic fields variation for this case have been shown in figures 5 (a) and (b) respectively. It is clear from figure 5 that in this case also the fields are non-uniform and asymmetrical. The oscillation frequency in this case is found to be 4.447 GHz for 2π-mode of oscillation and is shifted downward by 133 MHz as compared to A6 basic resonant structure.

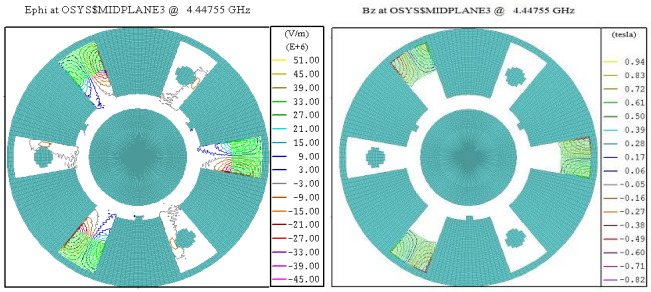

Figure 5: Azimuthal variation of (a) RF electric field (b) RF magnetic field for 2π-mode of oscillation with annular dielectric loaded RF resonators alternating 3 metal rods and protrusion

Next, PIC simulations have been carried out on both the structures for RF output power and oscillation frequency comparison. The anode voltage of 360 kV is applied at input port of the simulation model shown in figure 2(b). The resulting voltage is measured along a line created in radial direction at input port. The anode voltage measured (E.DL) is as shown in figure 6. The anode voltage is stabilized at 360 kV after 20 ns following some initial overshoots. The electron emission starts after 30 RF periods (~6.5 ns). After 10 ns the electron sheath around the cathode just start to interact with the wave over resonator, at the same time power also starts to grow slowly but due to multimode operation saturated power could not be achieved even after 60 ns. The output power comparison graphs for the cases of 3 metal rods with alternating annular dielectric loaded RF resonators and protrusions/recession with A6 basic structure is shown in figure 7(a).

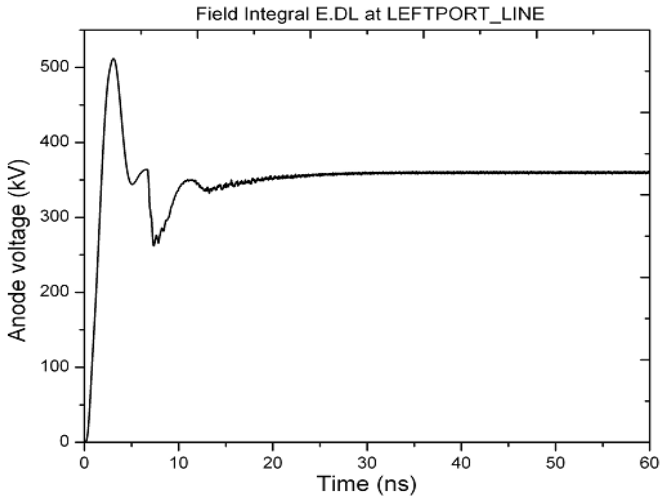

Figure 6: Anode voltage measured at input port.

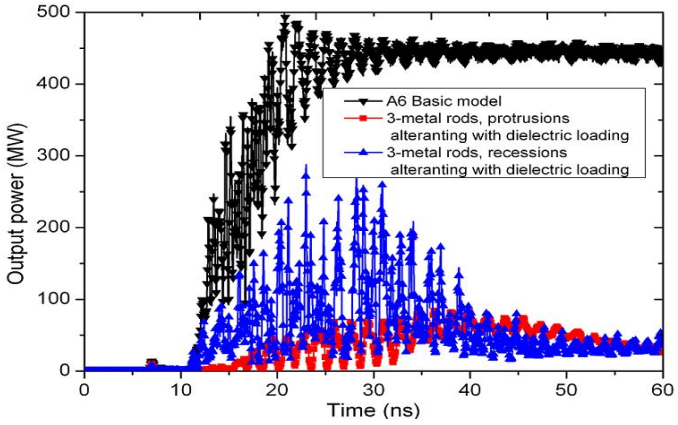

Figure 7 (a): Comparison of output power in the case of 3 symmetrical metal rods with alternating annular dielectric loaded RF resonators and protrusions/recessions.

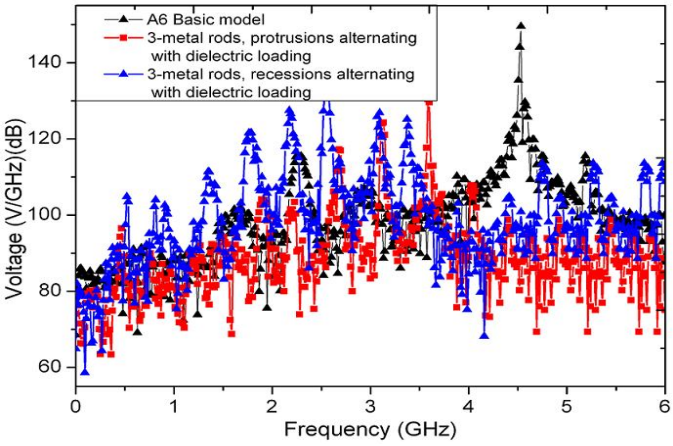

Figure 7(b): Comparison of oscillation spectrums in the case of 3 symmetrical metal rods with alternating annular dielectric loaded RF resonators and protrusions/recessions.

It is noticed that in the A6 relativistic magnetron loaded symmetrically with low loss annular dielectric material alternating metal rods in side resonators and protrusions / recessions along anode vanes inner surfaces stable operation is not possible due to multimode operation which can be confirmed from oscillation spectrum shown in figure 7 (b). The reason for this instability is the number of field variation created by metals rods, dielectric material, and protrusions/recessions. In this structure total number of field variation is nine, but for stable operation in 2π-mode of oscillation in a six vane magnetron should be six. Hence, it is expected that stable operation with improved output performance can be achieved with larger number of resonant cavities. Certainly, if we increase the number of resonators, the problem of multi-moding will increase, so some mode separation techniques, like strapped resonant structure or rising–sun resonant structure should be explored for relativistic case for stable operation with proper mode separation.

4. CONCLUSION

It is observed that in both the above cases, stable operation is not possible due to multimode operation which can be confirmed from oscillation spectrum. It is supposed in these cases that the maximum power is generated in π- and other competitive modes. A parametric analysis has also been carried out with respect to angular width of protrusion /recessions as well as radius of the metal rods, but stable power could not be achieved in any case. The reason for this instability as expected is the nine numbers of field variation created by metals rods, dielectric material, and protrusions/recessions, which do not support 2π-mode of operation in a relativistic magnetron having six numbers of vanes

ACKNOWLEDGEMENT

Authors are thankful to the Director, CSIR-CEERI for granting permission to publish this paper. Thanks are due to Dr. L. Ludeking at Mission Research Corporation for valuable discussions on MAGIC3D simulation techniques. They are also thankful to their colleagues of Project team for their supports.

REFERENCES

1. G.B. Collins. ***Microwave Magnetrons***, 1st ed. McGraw-Hill New York, 1948, ch. 1, pp. 1-10.
2. James Benford. ***High-Power Microwave Sources***, 2 nd ed., Artech House, Norwood, 1987, pp. 351-395.
3. Hae Jin Kim and Jin Joo Choi. **Three-dimensional particle-in-cell simulation study of a frequency tunable relativistic magnetron,** *IEEE Trans. on Dielectrics and Electrical Insulation*, Vol. 14, pp. 1045-1049, August 2007.
4. J.I. Kim, J.H. Won, and G.S. Park. **Electron prebunching in Microwave Magnetron by Electric Priming using Anode shape modification**, *Applied Physics Letters,* Vol. 86, pp. 171501-3, April 2005.
5. V.B. Baiburin and K.V. Kaminskii. **Effect of an Azimuthally Varying Magnetic Field on the Noise Level in a Multicavity Magnetron**, *Technical Physics Letters*, Vol.35, pp. 582-584, 2009.
6. V. Bogdan Neculaes, Michael C. Jones, Ronald M. Gilgenbach, Y.Y. Lau, John W. Luginsland, Brad W. Hoff, William M. White, N.M. Jordan, P. Pengvanich, Y. Hidaka, and Herman L. Bosman. **Magnetic Priming Effects on Noise, Startup, and Mode Competition in Magnetrons**, *IEEE Trans. Plasma Sci.*, Vol. 33, pp. 94-101, February 2005.
7. B.W. Hoff, Gilgenbach R.M., Jordan N.M., Lau Y.Y., Cruz E.J., French D.M., Gomez M.R., Zier J.C., Spencer T.A., Price D. **Magnetic Priming at the Cathode of a Relativistic Magnetron**, *IEEE Trans. Plasma Sci.* Vol 36, pp. 710-717, June 2008.
8. B. Neculaes, R.M. Gilgenbach, and Y.Y. Lau. **Low-noise microwave magnetrons by azimuthally varying axial magnetic field**, *Applied Physics Letters*, Vol. 83, pp. 1938-1940, September 2003.
9. Brad W. Hoff, Matthew Franzi, Ronald M. Gilgenbach and Y.Y. Lau. **Three-Dimensional Simulations of Magnetic Priming of a Relativistic Magnetron**, *IEEE Trans. Plasma Science*, Vol. 38, pp. 1292-1301, June 2010.
10. Mikhail I Fuks SM IEEE and Edl Schamiloglu. **70 % Efficient relativistic magnetron with axial extraction of radiation through a horn antenna**, *IEEE Trans. Plasma Science*, Vol. 38, pp. 1302-1312, June 2010.
11. S.M.A. Hashemi. **Dielectric cavity relativistic magnetron**, *Applied Physics Letters*, 96, pp. 0815031-3, February 2010.
12. Shivendra Maurya, V.V.P. Singh and P.K. Jain. **Study of Output Performance of Partially Dielectric loaded A6 Relativistic Magnetron**, *IEEE Trans. on Plasma Science.* Vol. 40, Issue 4, pp. 1070-1074, April 2012.
13. Shivendra Maurya, V.V.P. Singh and P.K. Jain. **Three-Dimensional particle-in—cell simulation of fast oscillation startup and efficiency improvement in a relativistic magnetron with electric priming**, *IEEE Trans. on Plasma Science*, Vol. 40, Issue 10, pp. 2686-2692, October 2012.
14. Bruce Goplen, Larry Ludeking, David Smithe, Gary Warren. **User-configurable MAGIC for electromagnetic PIC calculations**, *Computer Physics Communications*, Vol. 87, page 54-86, 1995.